ACTIVATED NANOCLAY IMPREGNATED STYRENE BUTADIENE RUBBER NANOCOMPOSITES: THERMAL TRANSPORT/DECOMPOSITION, THERMAL TRANSITIONS AND MECHANICAL PARAMETERS

Nadeem Iqbal[1*], Sadia Sagar Iqbal[2], Abdul Waheed Anwar[3], Samreen Mustafa[4], Sajid Rashid[5]

[1]Department of Polymer Engineering and Technology, CEET, University of the Punjab,Lahore, (Pakistan)
[2]School of Chemical & Materials Engineering, National University of Sciences & Technology, Islamabad, (Pakistan)
[3]Nanotechnologies Research Centre/Department of Physics, University of Engineering and Technology, Lahore, (Pakistan)
[4]Materials Synthesis Lab, School of Physical Sciences/Department of Physics, University of the Punjab, Lahore, (Pakistan)
[5]GIS, University of the Punjab, Lahore, (Pakistan)

ABSTRACT

In order to enhance the thermal insulation/stability and mechanical properties of the styrene butadiene rubber, four progressive concentrations of activated nanokaolinite were impregnated using conventional dispersion kneader and two roller mixing mill followed by hot isostatic compression molding to fabricate polymer nanocomposites. Nanoclay activation, particle size and crystallinity were confirmed performing FTIR, SEM/EDS, and XRD techniques. Thermal conductivity and thermal impedance of the composite specimens were carried out using ASTM standards. Thermal transport through the polymer nanocomposite was restricted with increasing nanoclay to matrix ratio and as a result thermal conductivity was reduced 41% while thermal impedance was elevated 30%. Thermal stability and endothermic capability were augmented with increasing filler concentration in the host matrix. DSC study reveals that the phase transition temperatures and their corresponding enthalpies were remarkably influenced with the filler incorporation into the polymer matrix. The ultimate tensile strength of the nanocomposites was elevated 83%, elongation at break 24% and modulus of elasticity 67% with the peak layered silicate mineral introduction into the SBR matrix. The morphological and compositional analyses of the thermal transport tested specimens were executed using scanning electron microscopy and energy dispersive spectroscopy, respectively.

Keywords: Nanoclays, Polymer-matrix composites (PMCs), Thermal properties, Transport properties, Thermogravimetric analysis (TGA), Thermal transitions

I. INTRODUCTION

The clays study has become a prominent topic of the present era due to their easy and abundant availability, low cost, and environment friendly nature. These clays have multidisciplinary applications, i.e., construction,

polymer, medicine, ceramic, and metal processing industries [1-3]. Montmorillonite, kaolinite, bentonite, etc were used in polymer matrices to enhance their thermal, physical, mechanical and fire retardant characteristics. Particle size of clay is an important parameter that influences the thermomechanical character of the base polymer. Nanoclays have several advantages over micro size clays due to their large surface area, nanoscale interaction with the polymeric chains and low density [4-6]. Kaolinite is an aluminosilicate mineral clay having layered structure used in paints, medicines, rubbers, ceramics, etc. Modified and unmodified nanokaolinite /polymer composites have excellent thermal stability, thermal resistance and mechanical strength. Functionalyzation of the incorporated filler enhances compatibility and interactive bonding strength with the polymeric molecular chains of the host matrix. Consequently, thermo-mechanical, electrical, magnetic, etc properties are tailored in more fascinating fashion compared to unmodified/polymer composites. Kaolinite clay turns itself into different phases in the progressively increasing heating environment but remain in silicate form up to high temperatures (≈1600^{o}C). Functionalyzed Nanokaolinite (FNK) with low density, high aspect ratio, large surface area and soft nature has affirmed the promising reinforcing effects if uniformly dispersed in the rubber matrices, i.e., ethylene propylene diene monomer rubber, styrene butadiene rubber (SBR), acronitrile butadiene rubber, neoprene rubber, etc [7-9].

SBR is a synthetic rubber, synthesized through emulsion or solution polymerization. It has good abrasion, aging and impact strength. The main application area of this rubber is tire, shoes and gasket industries. Usually carbon black is reinforced in the SBR rubber to attain the required level of mechanical strength but thermal resistance suffers with the incorporation of this filler [10-13]. During the tire operation, enormous heat is generated due to road friction which may degrade the mechanical characteristics of the rubber [14-17]. So, the filler that improves thermal endurance, thermal resistance and mechanical strength, synchronously is required for SBR to perform better during its usage [18].

Thermal conductivity, thermal impedance, thermal degradation, differential thermal analysis, differential scanning calorimetric study and mechanical properties were evaluated for FNK/SBR composites in this novel research. In addition, the effect of nanoclay (FNC) loadings on the glass transition, crystallization, melting temperatures and their associated specific enthalpies are also executed herein.

II. EXPERIMENTAL

2.1 Materials

Nanokaolinite, nanosilica, sulphur, zinc oxide and stearic acid were purchased from BDH. Mercaptobenzthiazole Disulphide (MBTS) and Cyclohexyl Benzthiazyl Sulphenamide (HBS) were supplied by Dalian Richon Chemical Co. Ltd, China. Aromatic oil and wax were received from International petrochemicals (Pvt) Ltd, Pakistan. Emulsified Styrene butadiene rubber (INDOPOL 1502) was bought from Evergreen Global Pte. Singapore**.**

2.2 Characterization

Scanning electron microscopy (SEM, JSM 6940A, Jeol, Japan) along with the energy dispersive spectroscopy was used to characterize the surface morphology of the activated nanoclay, filler dispersion in nanocomposite specimens, charred samples and their composition analysis. Thermal conductivity (λ_s) of the polymer nanocomposite specimens were carried out using ASTM E1225-99. Experimental setup design to evaluate λ_s of the composite specimens in the temperature range 323 to 523K is depicted in Fig. 1.

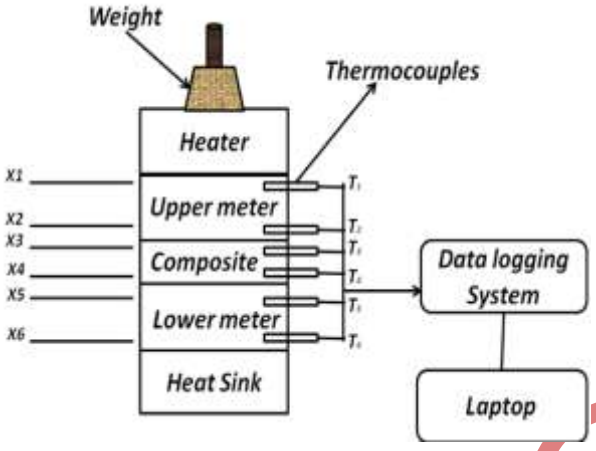

Figure 1. Experimental Setup Design to Execute Thermal Conductivity/Impedance of The Fabricated Rubber Nanocomposites

Schematic illustration of the comparative guarded longitudinal heat flow system shows the feasible locations of K-type thermocouples, heating source, water heat sink, temperature data logger, copper upper and lower meter bars and laptop [19]. Time–temperature profiles of all thermocouples located at specific positions were displayed on the laptop display using Squirrel OQ610 series temperature data logger. Thermal conductivity of the composite specimens was measured at different input temperatures using equation (1).

Thermal conductivity of specimen=$\lambda_s = ((Q'_T + Q'_B)(x_4 - x_3)/2(T_4 - T_3))$ (1)

Heat flow at the top bar = $Q'_T = \lambda_M * (T_2 - T_1)/(x_2 - x_1)$

Heat flow at the bottom bar =$Q'_B = \lambda_M * (T_6 - T_5)/(x_6 - x_5)$

T_1 , T_2 , T_3 , T_4 , T_5 , and T_6 are the temperatures of the six thermocouples and x_1 , x_2 , x_3 , x_4 , x_5 , and x_6 are their positions. λ_M is thermal conductivity of the copper bar.

Thermal impedance of a material is its ability to resist thermal/temperature fluctuations in a variable heating environment. For thermal impedance four thermocouples have been used instead of six in afore mentioned thermal conductivity design. Thermal impedance of the nanocomposite specimens were measured according to the ASTM D5470-03 and by following equation (2).

Thermal impedance (m^2-K/W) = $R = \lambda_M (T_A - T_D)*(Area/Q)$
(2)

Q = V (Voltage) x I (Current)

Temperature of upper bar surface in contact with the sample (K) = $T_a = T_2 - ((T_1 - T_2)*(x_b/x_a))$

Temperature of lower bar surface in contact with the sample (K) = $T_d = T_3 - ((T_3 - T_4)*(x_d/x_c))$

T_1 (K) = Upper temperature of upper bar T_2 (K) = lower temperature of upper bar

T_3 (K) = Upper temperature of lower bar T_4 (K) = Lower temperature of lower bar

x_a (m) = Distance between T_1 to T_2 x_b (m) = Distance between T_2 to S Sample

x_c (m) = Distance between T_3 to T_4 x_d (m) = Distance between Sample to T_3

Thermal degradation and endothermic/exothermic capability of the rubber nanocomposites were carried out using Perkin Elmer Diamond TG/DTA, Japan. Heating rate and temperature range during the thermogravimetric and differential thermal analyses was 10°C/min and 25-850°C, respectively. Perkin Elmer Diamond DSC, Japan was used to analyze the heat flow response of the polymer composites from -75 to 450°C to determine physical transformations such as phase transitions (glass, crystallization, and melting) and their specific enthalpies with a heating rate (10°C/minute). Both of these studies were performed in the air atmosphere. Tensile strength, elongation at break, and modulus of elasticity of the polymer nanocomposite specimens were executed using universal tensile testing machine (AG-20KNXD Plus, Shimadzu) according to the ASTM standard D412-98A.

2.3 Synthesis and Functionalyzation of Kaolinite

Silane coupling agent (SCA), 3-aminopropyl-trimethoxysilane (APTMS) along with cetrimonium bromide (CTAB) was used for the surface treatment to activate the clay (kaolinite). A specific amount of the unmodified clay was added in ultra pure water in a ratio 10:100 and the mixture was sonicated in ultra-sonication bath at 70°C and 40 KHz frequency for 30min. After that, 1wt% CTAB was inserted in the preset mixture followed by further sonication under similar conditions for next 30min. Subsequently, 5 volume% SCA was added in the mixture and sonicated it for next three hours. Consequently, magnetic stirring followed at 1000rpm for an hour with 90°C. The sonicated solution was diluted five times to maintain its pH at 7. Centrifuge (Centurion Scientific C2 series) at 4000rpm was used to recover the nano alumino-silicate clay. The nanokaolinite sample was dried for 12h at 80°C to eradicate moisture from the specimen. Fig. 2(a) shows the FTIR spectra of unmodified/modified kaolinite. The peaks at 2922.91, 2849.14, 1826.55, 1463.25, and 1232.73cm^{-1} indentifies the presence of trimethoxy silane moiety at the surface of nanoclay [20, 21].

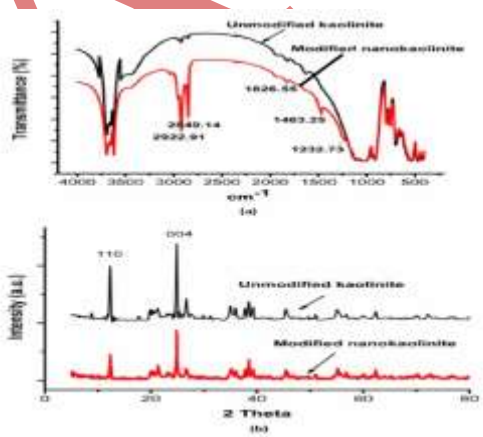

Figure 3. FTIR (A) And XRD (B) Patterns Of Unmodified/Modified Kaolinite

Experiment results reveals that the use of APTMS is the third stage is a goal practice to functionalize the nanokaolinite particles. Fig. 2(b) elucidates the diffraction band component analysis of the XRD patterns between 5-80° 2θ of both the untreated/treated kaolinite specimens. The diffraction peaks of untreated clay samples are narrow and intense, compare to the subsequent samples, indicating that the raw kaolinite specimen has a well ordered structure. The comparative analysis of both XRD patterns discloses that the ultrasonication

process in the presence of a surfactant and a silane coupling agent causes a progressive and general reduction of the peak intensity of all reflections located between 5-80^{o} 2θ. F. Franco et al [22] also endorses the above XRD explanation in his article. Fig. 3 shows the micrographs of unmodified and exfoliated modified clay at variant magnifications along with the compositional analysis of the kaolinite. The average particle size observed in Fig. 3(a) is 20µm for the untreated kaolinite. The synthesis and modification process has successfully reduced the particle size of the clay up to 1000 times. The average particle size noticed in Fig. 3(b) and 3(c) for treated/processed kaolinite is 15nm. Another interesting thing in the morphological analysis of the nanoclay is that all particles have approximately the similar spherical shape and size. Another advantage of this route is that both the nanoparticles synthesis and modification are taken place synchronously. The EDS analysis in Fig. 3(d), illustrates the presence of Al (21.05), Si (32.86), and O (46.09) present in nanokaolinite ($Al_2Si_2O_5(OH)_4$) that means synthesized nanoparticles maintain their original composition (untreated clay).

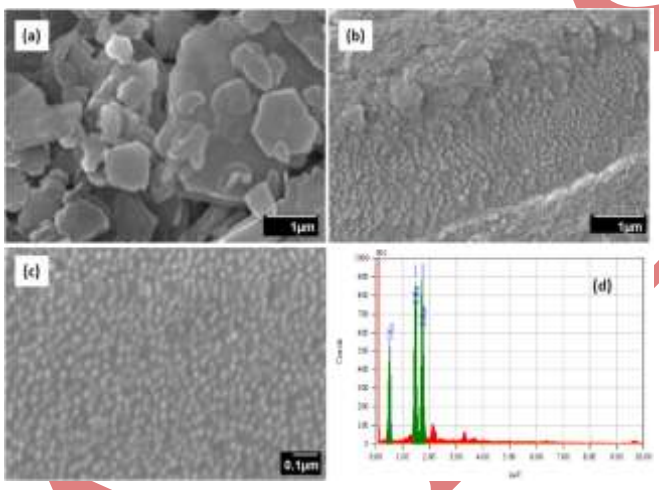

Figure 3. Surface morphology of unmodified (a), and modified (b, c) clay along with its compositional analysis (d)

2.4 Fabrication of FNK/SBR Nanocomposites

A preset amount of nanosilica (reinforcement), aromatic oil (lubricant), wax (lubricant), stearic acid (surface modifier of the nanoclay) and four progressive loadings (0–30wt %) of FNK were inserted in the dispersion kneader chamber along with the SBR matrix at 110^{o}C for 30 minutes to disperse nanofillers properly in the host matrix. Sulphur (cross linker), MBTS (primary accelerator), HBS (secondary accelerator), and zinc oxide (activator) were incorporated into the rubber matrix in the post mixing stage on a two roller mixing mill at 60^{o}C and 30rpm roller's speed for twenty minutes to disperse the reinforcements and processing aids homogeneously within the polymer matrix [23]. Table 1 illustrates the basic composition of SBR composite (SC1). The four nanoclay concentrations, i.e., 0–30 wt%, each composite formulation had a difference of 10 wt%, were impregnated in the rubber matrix and the four rubber compositions are nominated as SC1, SC2, SC3, and SC4, correspondingly. The base formulation of the polymer nanocomposite is SC1 and is illustrated in Table 1.

III. RESULTS & DISCUSSION

3.1 Thermal Conductivity and Thermal Impedance analyses

Thermal conductivity contours of the rubber nanocomposites in the temperature range 323 to 523K are illustrated in Fig. 4. Initially, thermal conduction through the SC1 composite is minimum compared to the clay nanocomposites.

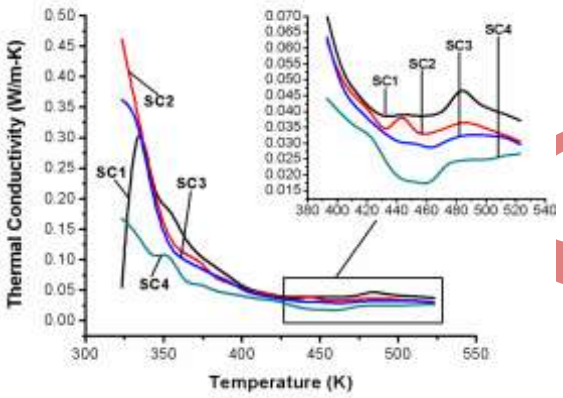

Figure 4. The Effect of Nanoclay on Thermal Conductivity of the SBR Nanocomposite with Four Diverse Loading Concentrations

A drastic decline is observed in the λ_s values of the composite in the temperature range (TR) 333–373K, after that each rubber nanocomposite has established a separate level of λ_s in the proceeding TR. The SC4 nanocomposite having 30 wt% FNK, has the least level of λ_s due to enormous heat quenching by the nanoclay during its phase changes and water evaporation. The variation of λ_s with respect to the NK inclusions is displayed in Fig. 5. It elucidates that λ_s is diminished with the progressive addition of NK in the rubber matrix. The utmost NK loaded nanocomposite formulation has 41, 22, and 41% less λ_s compared to 0 wt% concentrated SC1 composite specimen at 373, 423, and 473K, respectively due to the high surface area, excellent heat absorbing capability, and nanoscale interaction of NK with the polymer matrix [24-26]. Functionalyzation and water of crystallization present in the nanoclay also impart an important role to quench enormous heat and consequently reduces the thermal conductivity of elastomeric nanocomposites.

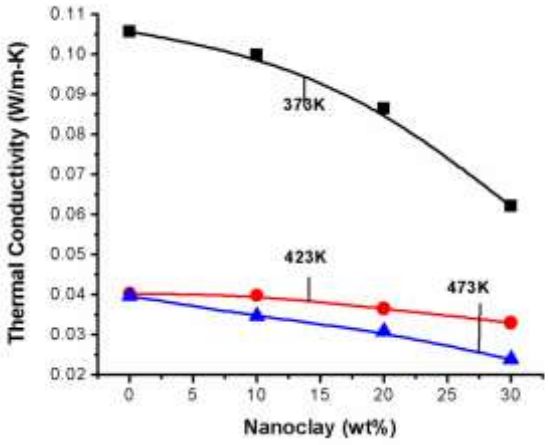

Figure 5. The Variation of Thermal Conductivity with the Progressive Addition of Nanoclay in the SBR Matrix at Three Diverse Temperatures

Thermal impedance (R) is an important characteristic of a polymer composite which ensures the capability of a material to resist thermal variation encounter during a specific application. Fig. 6 simulates the effect of FNK on the thermal impedance of the nanocomposite specimens. An elevation in R values up to 493K is observed in the graph and then a reduction is scrutinized in the further temperature line due to transpirational cooling effect associated with evaporation of aromatic oil within the nanocomposite specimens. The nanocomposite SC4 has the maximum ability to resist incoming heat flux within the complete tested temperature range due to the maximum nanoclay incorporation into the polymer matrix [22, 27].

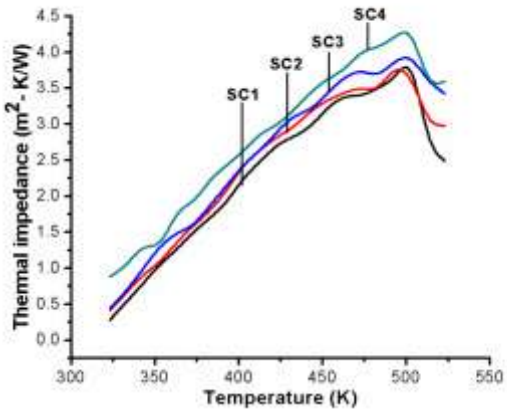

Figure 6. The Effect of Nanokaolinite on the Thermal Impedance of the Rubber Nanocomposites in the Temperature Range 323K-523K

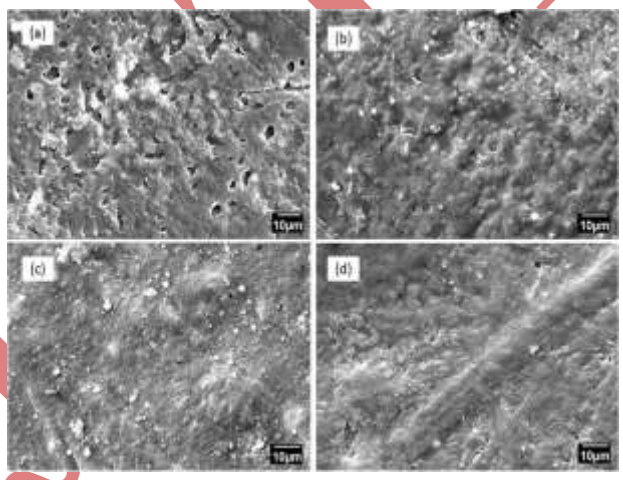

Figure 7. SEM Micrographs of the Post Thermal Conductivity Tested SC1 A), SC2 B), SC3 C), and SC4 D) Rubber Nanocomposites

Fig. 7 (a), (b), (c) and (d) simulates the surface morphological analysis of the post thermal conductivity tested nanocomposite specimens in the temperature range 323 to 523K. A large number of micro-voids are observed in SCI while the size and quantity of theses pores are remarkably reduced with increasing FNK concentration in the rubber matrix. It means that nanoclay impregnated rubber nanocomposites has less surface rupture in the heating environment compared to the base polymer due to the excellent thermal stability and heat absorbing capability on the nanoclay.

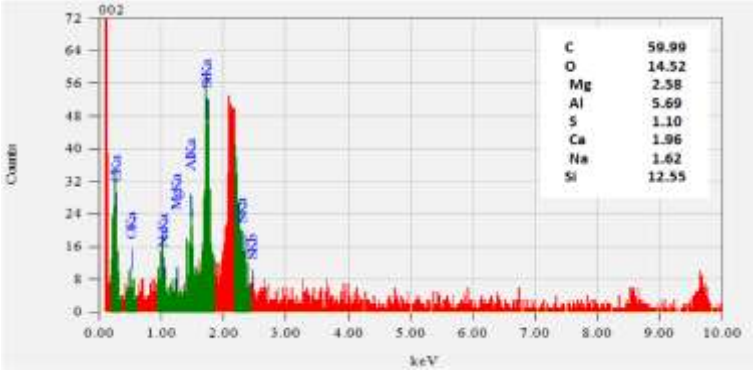

Figure 7e. The compositional analysis of 30 wt% loaded composite specimen

Fig. 7e elaborates the compositional analysis of the 30wt% loaded rubber composite. The elements C (59.99%), Al (5.69%), Si (12.55%), O (14.52%), S (1.10%), Ca (1.96%), Mg (2.58%) and Na (1.62%) are found in the energy dispersive spectroscopic analysis of the polymer nanocomposite that confirmed the incorporated filler impregnation in the host polymer matrix.

3.2 Thermal Decomposition of the Nanocomposites

Thermal endurance of the rubber nanocomposites were analyzed in air atmosphere from room temperature to 850°C and portrayed in Fig. 8.

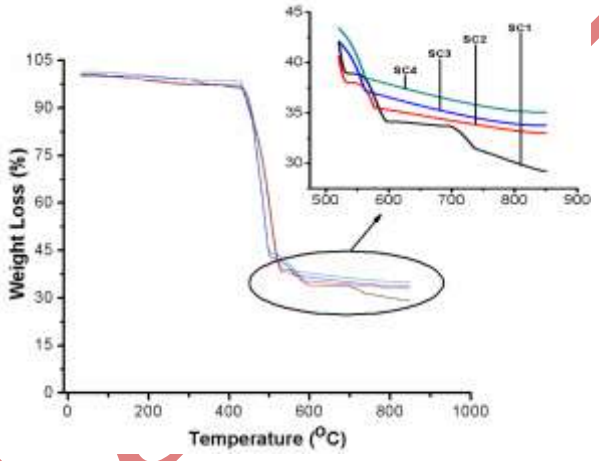

Figure 8. Thermal Degradation Analysis of the Nanokaolinite Impregnated SBR Nanocomposites in the Temperature Range 25 – 850°c in Air Environment

An insignificant weight loss is observed up to 425°C and then the maximum thermal degradation is scrutinized in the proceeding 100°C due to polymer pyrolysis and polymeric molecular chain cession. From 550 to 850°C, there is no significant change in weight loss is observed for the nanocomposite specimens due to the remaining carbon char and the nano-inclusion. A momentous enhancement in thermal endurance is noticed at all temperatures with the FNK concentration elevation in the SBR matrix [27, 28].

3.3 Differential Thermal analysis

Fig. 9 demonstrates the heat quenching potential of the FNK/SBR nanocomposite. The composite specimens absorb enormous heat 300°C and the upward plateaus are observed 600°C due to the exhaust of volatile products

included in the rubber nanocomposites. The heat absorbing capability of the nanocomposites is augmented with the progressive incorporation of NK in the rubber matrix due to the excellent thermal stability, high surface area, and nanoscale interaction of the nanoclay with polymeric molecular chains [29].

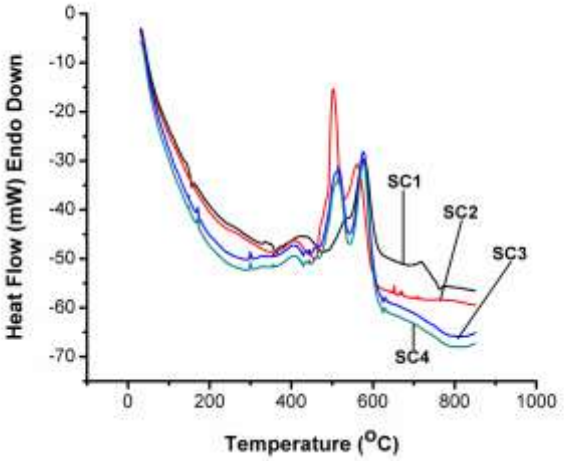

Figure 9. Thermal absorbance capability of the rubber nanocomposites in the temperature range 25–850°C

3.4 Differential Scanning Calorimetric Study

Fig. 10 illustrates the DSC analysis of the rubber nanocomposites in the temperature range -74 to 450°C to analyze the effect of nanoclay concentration on the phase transition temperatures and their specific enthalpies. Glass transition temperature (T_g), crystallization temperature (T_c), first melting phase temperature (T_{m1}), and second melting phase temperature (T_{m2}) of the FNK/SBR nanocomposites are compiled in Table 2.

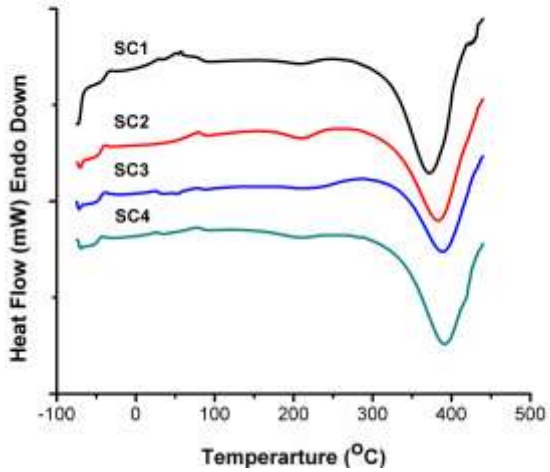

Figure 10. DSC Curves of the Nanocomposite Specimens in the Temperature Range -74 To 450°c

The Glass transition temperature (T_g) of the polymer nanocomposites is reduced with increasing filler concentration in the host matrix and a 10°C T_g reduction is noticed with the 30 wt% incorporation of FNK in the rubber matrix. It means that the nano inclusion remarkably enhances the rubber phase of SBR nanocomposite by interacting with polymeric molecular chains at the nanoscale, reducing the crosslinking density of the base polymer that eventually enhances the plasticity of the host polymer matrix. Crystallization temperature of the SC4 nanocomposite is less than the SC1 composite owing to the excess FNK loading in the former mentioned

formulation. The progressive addition of the nanoclay has reduced the T_c of the composite specimens due to the crystalline nature of the FNK. The effect of the filler concentration on the melting characteristics of the rubber nanocomposite is opposite to T_g and T_c. The melting temperatures T_{m1} and T_{m2} were promoted and the utmost concentration of FNK elevates T_{m2} 19^{o}C due to high thermal stability, heat absorbing capability, surface area and even dispersion of the nanoclay in the host polymer matrix [30-32]. Thermal phase transitions with increasing temperature resulted to quench enormous heat and high melting temperature of the fabricated nanocomposite. The specific enthalpies of glass transition temperature and crystallization temperature phases were diminished while a significant evolution was noticed in the first and second melting phase transitions due to the surplus heat absorbing capacity of the FNK. The SC4 nanocomposite has 74J/g more specific enthalpy compared to the SC1 formulation due to higher concentration of the reinforcing filler in the aforementioned composition compared to afterward, counterpart.

3.5 Mechanical Properties

The stress–strain contours of the polymer nanocomposites are displayed in Fig. 11(a), which simulates a remarkable evolution in toughness of the composite specimens with increasing filler incorporation into the rubber matrix. The effect of NK loading on the tensile strength, elongation at break, and modulus at 100% elasticity of the fabricated composite formulations is compiled in Fig. 11(b).

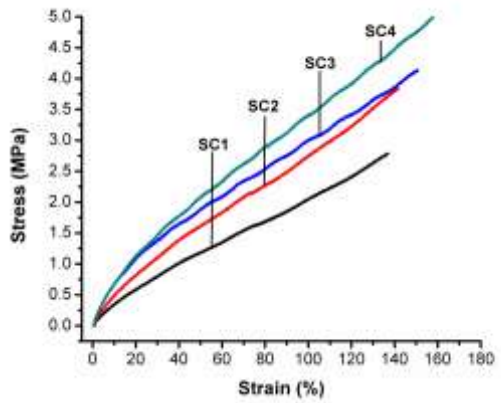

Figure 11a. Stress–Strain Contours of the Nanoclay/SBR Nanocomposites

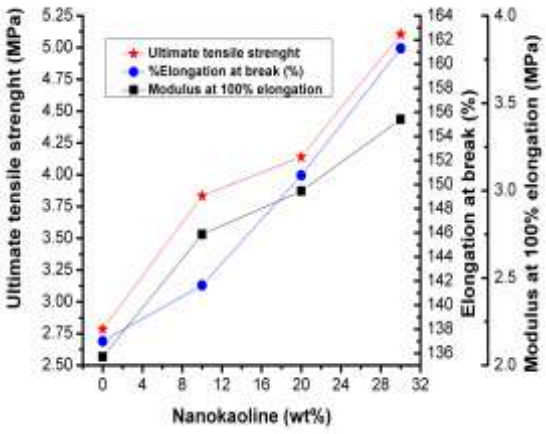

Figure 11b. The Effect of Nanokaolinite Concentration on the Ultimate Tensile Strength, Elongation at Break, And Modulus 100% Elasticity of the Rubber Nanocomposites

The ultimate tensile strength is progressed from 2.78 to 5.10MPa, elongation at break is elevated from 137 to 161, and modulus of elasticity at 100% elongation is promoted from 2.04 to 3.40Mpa with the 30 wt% addition of the nanoclay in the polymer matrix due to the high surface area, layered structure, even dispersion, and nanoscale interaction of the nanofiller with the polymeric molecular chains of the host matrix. Shore A hardness comparison of the rubber nanocomposites is displayed in Fig. 11(c) [33, 34]. Shore A hardness is augmented from 46 to 56 with the 30 wt%, respectively progressive impregnation of nanokaolinite in the SBR base formulation (SC1 nanocomposite). The FNK introduction into the host polymer matrix reduces the chain mobility and consequently enhances the rubber hardness of the developed elastomeric composite [35, 36].

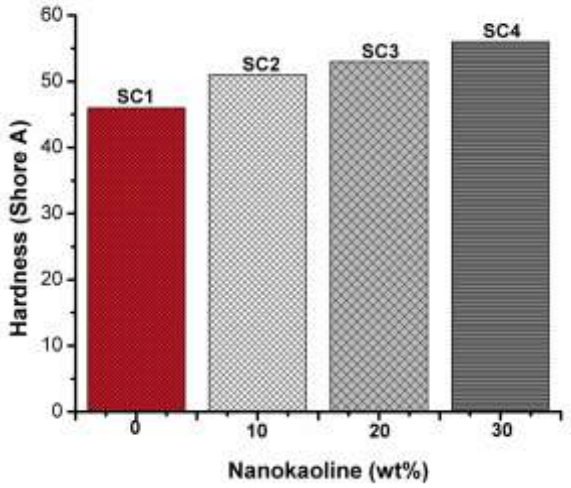

Figure 11c. Shore A Hardness Of The Polymer Nanocomposites With Diverse Nanoclay Loadings.

IV. CONCLUSION

Functionalyzed nanoclay was synthesized and characterized. Activated nanokaolinite is evenly dispersed in the styrene butadiene rubber matrix using dispersion kneader and two roller mixing mill. Thermal conductivity of the rubber nanocomposites is reduced up to 41%; thermal impedance is elevated 41%; thermal stability is promoted 5%; glass transition and crystallization temperatures are diminished 10 and 3^{o}C, respectively; first and second melting phase temperatures are increased 1.5 and 19.7^{o}C, correspondingly; ultimate tensile strength, rubber hardness, elongation at break, and modulus of elasticity at 100% elongation are augmented 2.37MPa, 10 Shore A, 24%, and 1.3MPa, respectively with 30 wt% nanoclay impregnation in the base composite formulation. Heat absorbing capability and toughness of the polymer nanocomposites are remarkably enhanced with the progressive incorporation of the nanofiller in the host rubber matrix. SEM analysis of the post thermal transport tested specimens reveals the micro- void's size and quantity reduction with increasing filler to matrix ratio.

ACKNOWLEDGEMENTS

The authors would like to greatly acknowledge Longman mills Lahore and Higher Education Commission of Pakistan for providing facilities regarding fabrication of rubber nanocomposites and financial support, respectively.

REFERENCES

[1] Bahramian, A.R., High temperature ablation of kaolinite layered silicate/phenolic resin/asbestos cloth nanocomposite, Journal of hazardous materials, 150 (2008)136.

[2] Conzatti, L., The clay mineral modifier as the key to steer the properties of rubber nanocomposites, Applied Clay Science, 61 (2012)14

[3] Díez, J., Exfoliated/intercalated silicate/hot styrene butadiene rubber nanocomposites: Structure properties relationship, Journal of Applied Polymer Science, 125 (2012)705.

[4] Kaneko, M.L.Q.A., High molar mass silicone rubber reinforced with montmorillonite clay masterbatches: Morphology and mechanical properties, European Polymer Journal, 46 (2010)881.

[5] Salehi, M. and M. Razzaghi-Kashani, Comparing styrene butadiene rubber–clay nanocomposites prepared by melt intercalation and latex-coagulation methods, Journal of Applied Polymer Science, 126 (2012) 253.

[6] Vijayan, P.P., Effect of nanoclay and carboxyl-terminated (butadiene-co-acrylonitrile)(CTBN) rubber on the reaction induced phase separation and cure kinetics of an epoxy/cyclic anhydride system, Journal of Materials Science, 47 (2012). 5241

[7] Al-Safy, R., Experimental investigation on the thermal and mechanical properties of nanoclay-modified adhesives used for bonding CFRP to concrete substrates, Construction and Building Materials, 28 (2012)769

[8] El-Sabbagh, S., N. Ahmed, and A. Ward, Effect of kaolin–metal oxides core–shell pigments on the properties of styrene–butadiene rubber composites, Materials & Design, 40 (2012) 343.

[9] Panda, A.K., Effect of sulphuric acid treatment on the physico-chemical characteristics of kaolin clay, Colloids and Surfaces A: Physicochemical and Engineering Aspects, 363 (2010) 98.

[10] Chen, S., Thermal degradation behavior of hydrogenated nitrile-butadiene rubber (HNBR)/clay nanocomposite and HNBR/clay/carbon nanotubes nanocomposites, Thermochimica Acta, 491 (2009) 103

[11] Noriman, N., H. Ismail, and A. Rashid, The effects of trans-polyoctylene rubber on thermal analysis and fatigue properties of styrene butadiene rubber/recycled acrylonitrile butadiene rubber, Advances in polymer Technology, 31 (2012)100.

[12] Salgueiro, W., Temperature dependence on free volume in cured natural rubber and styrene butadiene rubber blends, Phys Rev E Stat Nonlin Soft Matter Phys, 83 (2011) 51.

[13] Wang, Q., W. Gao, and L. Zhang, Research of styrene-butadiene rubber/silicon-aluminum oxides nanotube binary nanocomposi, Journal of Applied Polymer Science, 120 (2011) 3196.

[14] Lei, Y., Thiol-containing ionic liquid for the modification of styrene–butadiene rubber/silica composite, Journal of Applied Polymer Science, 123 (2012) 1252.

[15] Tian, M., Overall properties of fibrillar silicate/styrene–butadiene rubber nanocomposites, Journal of Applied Polymer Science,. 101 (2006) 2725.

[16] Zanchet, A., Use of styrene butadiene rubber industrial waste devulcanized by microwave in rubber composites for automotive application, Materials & Design, 39 (2012) 437.

[17] Zhang, H., Toughening of polylactide by melt blending with methyl methacrylate–butadiene–styrene copolymer, Journal of Applied Polymer Science, 125 (2012) 550.

[18] De Falco, A., Accelerator adsorption onto carbon nanotubes surface affects the vulcanization process of styrene–butadiene rubber composites, Journal of Applied Polymer Science, 113 (2009) 2851.

[19] Zhou, X., Y. Zhu, and J. Liang, Effects of the vulcanizing reagent addition on the properties of CNTs/SBR powder composites, Journal of Applied Polymer Science, 106 (2007) 1836.

[20] Iqbal, N., Fabrication and characterization of multiwalled carbon nanotubes/silicone rubber composites, Journal of Applied Polymer Science, 128 (2013) 2439.

[21] Yau, Y.H., H.F. Wong, and N. Ahmad, Numerical heat transfer study for a large rubber product, International Journal of Heat and Mass Transfer, 55 (2012) 2879.

[22] Franco, F., Particle-size reduction of dickite by ultrasound treatments: effect on the structure, shape and particle-size distribution, Applied clay science, 35 (2007) 119.

[23] Mu, L., The effect of thermal conductivity and friction coefficient on the contact temperature of polyimide composites: Experimental and finite element simu lation, Experimental and finite element simulation. Tribology International, 53 (2012) 45.

[24] Ko, Y.J., Poly (amic acid) Treatment on BaTiO3 and Effect on the Dielectric Properties of BaTiO3/Polyimide Composites, Advanced Materials Research, 560 (2012) 880.

[25] Li, Z., Study on thermally conductive ESBR vulcanizates, Polymer Bulletin, 67 (2011)1091.

[26] Vandenberg, E.T., Structure of 3-aminopropyl triethoxy silane on silicon oxide, Journal of Colloid and Interface Science, 147 (1991) 103

[27] Ali Raza, M., Effect of nanosized carbon black on the morphology, transport, and mechanical properties of rubbery epoxy and silicone composites, Journal of Applied Polymer Science, 126 (2012) 641.

[28] Liu, K., Effect of lumen size on the effective transverse thermal conductivity of unidirectional natural fiber composites, Composites Science and Technology, 72 (2012) 633.

[29] Yu, H., Thermal and insulating properties of epoxy/aluminum nitride composites used for thermal interface material, Journal of Applied Polymer Science, 124 (2012)669.

[30] Cibulková, Z., et al., Stabilization effect of potential antioxidants on the thermooxidative stability of styrene–butadiene rubber, Journal of Thermal Analysis and Calorimetry, 105 (2011) 607.

[31] Taşdemir, M. and E. Uluğ, Mechanical, morphological and thermal properties of SEBS, SIS and SBR-type thermoplastic elastomers toughened high impact polystyrene, Polymer-Plastics Technology and Engineering. 51 (2012) 164.

[32] Zulkepli, N.N. and H. Ismail, A study of FTIR, thermal properties and natural weathering test on NBRvirgin/recycled with SBR blends, Polymer-Plastics Technology and Engineering, 51,350 (2012).

[33] Cibulková, Z., et al., DSC study of stabilizing effect of antioxidant mixtures in styrene-butadiene rubber, Journal of thermal analysis and calorimetry, 108, 415 (2012).

[34] Jayasree, T. and P. Predeep, Non-isothermal crystallization behavior of Styrene butadiene rubber/high density polyethylene binary blends, Journal of thermal analysis and calorimetry, 108, 1151 (2012).

[35] Qu, L., et al., Effect of filler–elastomer interactions on the mechanical and nonlinear viscoelastic behaviors of chemically modified silica-reinforced solution-polymerized styrene butadiene rubber, Journal of Applied Polymer Science, 126 (2012) 116

[36] Vasilakos, S. and P. Tarantili, Mechanical properties and nanostructure correlation of condensation-type poly (dimethyl siloxane)/layered silicate hybrids, Journal of Applied Polymer Science, 125 (2012) 548.